RESEARCH PAPER

SDS Capped CdTe QDs Binary Mixture for Dye-sensitized Solar Cell Applications

Ameer Qasim Abd *, Odai N. Salman

Applied Sciences Department, University of Technology- Iraq, Baghdad, Iraq

ARTICLE INFO

ABSTRACT

The creation of Semiconductor Quantum Dots (QDs) utilizing the pulsed Laser ablation approach from a solid target in a liquid media is simple, rapid, and has a lower environmental effect than other methods. The synthesis of sodium dodecyl sulfate (SDS) capped Cadmium telluride (CdTe) The morphological and optical characteristics of the prepared CdTe QDs were investigated by X-ray diffraction, UV-Vis spectra, Fourier Transform infrared spectroscopy; and transmission electron microscopy. QDs ranging in size from 3 nm to 12 nm were seen to develop. The log normal distribution is used to describe the distribution of particle diameter. The short-circuit current density rose by 20% in the dye sensitized solar cell (DSSC) with and without SDS capped CdTe QDs. and the solar cell efficiency augmented from 0.58 to 1.10%.

How to cite this article

INTRODUCTION

Energy consumption is expected to climb by 54% by 2036 as a result of economic expansion and strong population growth [1]. Solar energy has risen steadily in recent years, as have mineral energy sources, which will almost definitely be exhausted in the next 50 years. The energy that falls from the sun to the earth is tremendous. It is projected to be 3×10^{24} J/year, or 10^4 times the amount used by humans. In other words, it will just cover 0.1% of the soil with a 10% productivity to meet current demands [2]. Quantum dots are semiconductor nanocrystals that are tiny enough to limit the travel of electrons in all three dimensions [3]. Due to its adaptable optical characteristics, Nano crystal solar cells containing QDs have seen considerable use in recent years

[4]. Quantum dots (QDs) are frequently used in electrical and optoelectronic applications, such as dye sensitized monocrystalline solar cells, which were invented by Organ and Gratzed in 1991[5]. Development on QDs and monocrystalline solar cells has accelerated in recent years. As a photosensitizer material, QD semiconducting materials are employed in such investigations to create electrons from solar radiation. One of the most significant advantages of QDSSCs is the ability to employ the desired area of the solar spectrum by altering the energy band gap of the light absorbing material. Until date, several different types of QD semiconductor materials have been employed as photosensitizer materials for QDSSC, with CdTe being one of them.[6] CdTe QDs have piqued the interest of researchers not only for their potential

* Corresponding Author Email: as.20.66@grad.uotechnology.edu.iq

utility in clarifying physical chemistry processes[7], but also for sensors, photo electrochemical (PEC) solar cells, optoelectronic devices, bio-labelling, bio-imaging, and gamma ray detectors, among other applications.[8] Several physical and chemical techniques are used in the manufacture of CdTe QDs. These methods are classified into two categories: top-down and bottom-up approaches. The bulk materials in the top-down technique begin to reach the nanostructures by (drilling, mechanical grinding, microwave, and spraying). The ascent begins with the molecule or atom and progresses to the nanoscale structure (co-precipitation, pyrolysis, vapor deposition, colloidal solution gel phases, atomic condensation and aerosol process) [9,10] Laser ablation is a typical example of the top-down technique in QDs synthesis. The pulsed laser ablation (Nd-YAG), discovered in 1964, is regarded as a very important type of laser. Pulsed laser ablation in liquid (PLAL) medium is an encouraging approach for controlling nano-materials production by quick reactive extinguishment of the ablated species at the liquid-plasma interface. Limited research has combined the pulsed laser ablation (PLA) approach into the manufacturing of CdTe QDs. The basic idea behind such research is to investigate the structure and optical characteristics of CdTe NPs manufacturing prepared employing PLA (Nd-YAG). Pulsed laser ablation (PLA) may manufacture more pure NPs with a virtuous crystalline structure that are affordable, safe, non-toxic, and environmentally beneficial [11].

In this paper, Pulse Laser Ablation was employed in this study to create CdTe QDs from an SDS-CdTe bulk solution. The optical and structural characteristics of CdTe NPs films formed on a glass substrate using the drop-casting approach were investigated in this work. Transmission Electron Microscopy (TEM) and XRD were used to investigate the crystallinity of the samples created, as well as the surface morphology. Photoluminescence (PL) tests, a UV-VIS spectrophotometer, and Fourier transforms infrared spectroscopy were used to assess their optical characteristics (FTIR). The solar cell was also tested. To the best of our knowledge, this is the first time using SDS capped CdTe quantum dots a stabilizing agent and Novel comparison study between DSSCs with and without SDS-capped CdTe QDs and prepared cdTe QDs by an easy and simple method is pulsed laser ablation.

MATERIALS AND METHODS

Anionic Powder containing Sodium dodecyl sulfate denoted as SDS hereafter; chemical formula is $NaC12H25SO4$ (Kanto Chemical Co., Inc.), purity 96 % and M.W. = 288.372 g/mol, as a surfactant (anionic detergent) [13], to examine the effect of the SDS concentrations on Surface Plasmon Resonance (SPR) in CdTe nanoparticles, we prepared different SDS solution with concentration (5mM) sample. The critical micelle concentration (CMC) of sodium dodecyl sulfate (8 mM). The SDS capped CdTe QDs were produced via laser ablation (1064 nm, 6 Hz, and pulse energy 200 mJ) of a CdTe bulk target. In the suspended liquid, utilizing Nd:Yag laser (kind Huafei), at 200 mj energy, 400 pulses; the sample of CdTe was immersed into the SDS via 3cm, where the space between the sample and the laser was 5 cm. Then Then an FTO slide was used, using the screen printing method on the conducting side of the FTO glass. TiO_2 paste was then applied (the mean nanoparticle size (active) was about 20 nm), and it was flattened with a razor onto. FTO slide (TCO30-10, SOLARONIX, with 10 ohm/ sq) leading to the development of a TiO_2 layer [14]. After dehydration, the TiO_2/FTO was added to the furnace. The resulting film was then annealed for an hour at 500°C. The film was cooled to room temperature before to the stage of immersion in the dye solution. The two TiO_2/FTO films were created using a similar process. For one day, TiO_2 electrodes were submerged in dye solutions (CdTeNPs-N719 dye as well as dye merely) [15]. Moreover, the platinum was produced using the oil-based platinum paste was dropped onto the FTO and then distributed with a blade. After the paste had dried, the paste was burned at 450°C. The results were homogeneously disseminated into platinum, which helped to give increased transparency and catalytic action. Additionally, the TiO_2/FTO/dye electrode was taken out of the liquids and rinsed with ethanol. Additionally, two holes were made in the counter electrode using a tiny diamond drill (DC12v/0.8A, Pros kit PK-500) in order to inject the tri-iodide electrolyte and iodine as a redox pair. In addition, organic iodide salt (I-/I_3-), imidazole molecule, and 3-methylpropionitrile have been added. Additionally, the next step entails positioning the hot melt tape on the TiO_2/dye electrode for pasting with platinum electrodes using a heating tool for 10 minutes at a temperature of 150°C. After that, many drops of

3methoxypropionitrile iodide salt, organic solvent, iodide salt, and imidazole compound were dropped into one hole to remove the bubbles from the other hole. Fourier Transform Infrared Spectroscopy (FTIR), Transmission Electron Microscopy (TEM) pictures, X-ray analysis in (lab XRD-6000, ADVANCEX-RAYSOLUTIONS-D8), and UV-Vis beam spectrophotometer have all been used to assess the properties of QDSSC (SP-3000 puls, optima Tokyo, Japan).

RESULTS AND DISCUSSION

The data of XRD of the CdTe Quantum dots film prepared by drop casting of NPs suspension dried on clean microscope slide recorded in the range (20°-50°) angle (See Fig. 1) displays the (111), (220), and (311) orientations at 2θ angles 23.8°, 39.6°, and 47.1°, respectively. The measured interplanar spacing (d_{hkl}) was obtained (3.51 Å) well-matched with those of the bulk cubic Zinc Blende (ZB) CdTe (d_{111} = 3.51Å for ZB CdTe, ICDD 01-057-2086). The crystallite size (D) of NPs can calculate with help from Scherrer equation (1) [16,17].

$$D = \frac{K\lambda}{\beta cos\,\theta} \qquad (1)$$

Where, k, λ, β, and θ represent the shape factor (0.9), the wavelength (0.15406 nm) of X-ray, FWHM of diffraction peak, and Bragg angle, respectively.
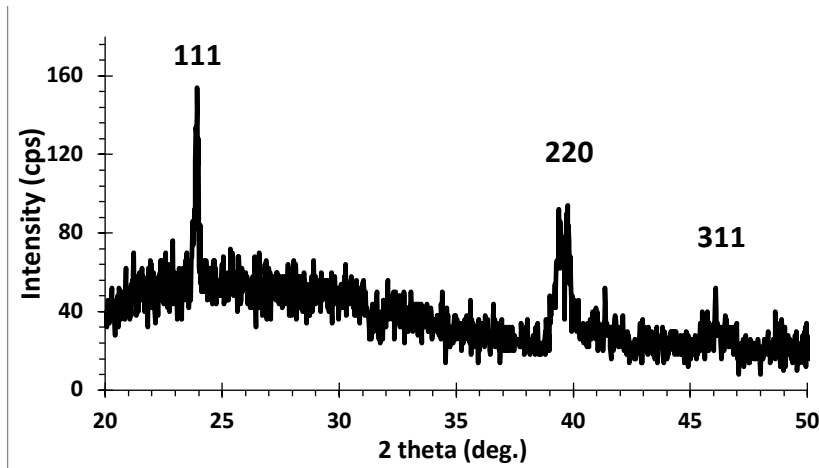

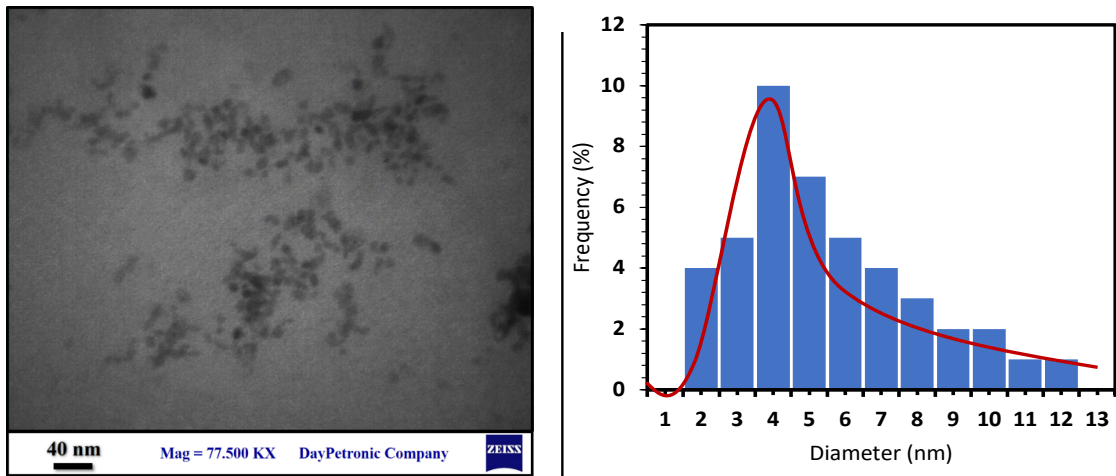Fig. 1. XRD pattern of the SDS capped CdTe quantum dots.

Fig. 2. (a) TEM image and (b) CdTe QDs size distribution

The averaged crystallite size D is about 8 nm in (111) orientation.

Fig. 2(a) shows a (77.500kX) magnified image of a colloidal liquid with SDS caps made of CdTe quantum dots and transmission electron microscope (TEM). Evidently, the formation the form of CdTe QDs is spherical. The distribution of size chart shown in Fig. 2(b), where the median particle diameter is approximately 4 nm, Better than what the researchers obtained in this research [18] shows how the sizes of CdTe quantum dots were matched and were fitted using a log-normal curve.

The optical band-gap of QDs NPs can be estimated using equation (2): [19]

$$\alpha h\nu = A(h\nu - E_g)^{1/2} \tag{2}$$

Where, hv: Energy of photon, α: Coefficient absorption, A: Constant, and E_g: The optical band-gap.

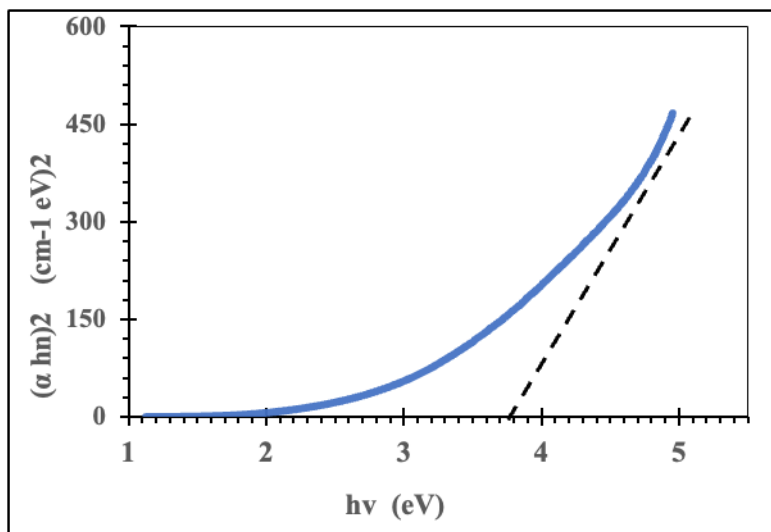Fig. 3 uses comparable data from the absorption spectrum to illustrate the Tauc plot for colloidal

Fig. 3. The optical band-gap of colloidal SDS capped CdTe quantum dots.
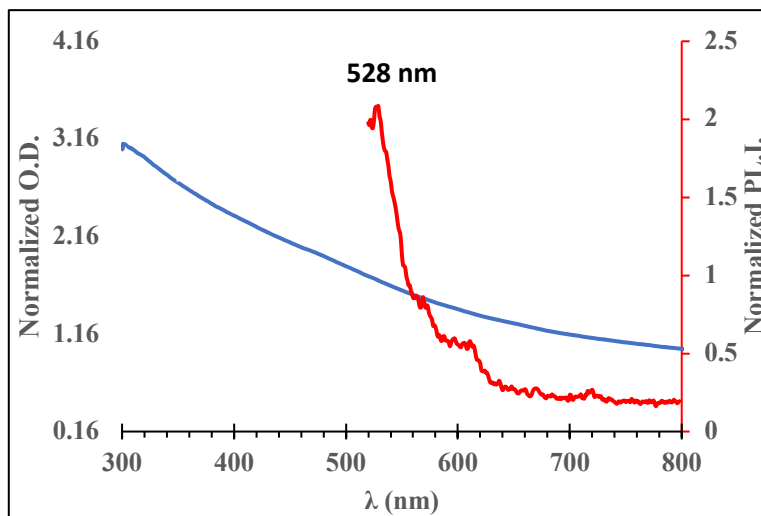

Fig. 4. Normalized Photoluminescence spectra and absorption spectra (excitation emission at 450 nm) for SDS capped CdTe quantum dots

CdTe quantum dots. Additionally, the intercept with the h-axis revealed that the optical energy gap (Eg) for the colloidal CdTe quantum dots was around (3.7 eV), and this finding is comparable to those of other studies.[7]

Fig. 4 elucidates the regularized optical density and the spectra of the emission of SDS capped CdTe QDs, and the narrow emission spectra localized at 528 nm resulted from the free exciton emission. Also, the share of electro-static interaction is between oppositely charged QD-SDS couple behind the perceived spectral variations in the binary mix. [12]

Fig. 5. FTIR For the confirmation of capping of SDS surfactant on CdTe nanoparticles. FTIR transmittance were reported for pure SDS, SDS capped CdTe a The peaks at 2853.32 and 2922.74 cm^{-1} corresponding to symmetric and asymmetric stretching CH$_3$ vibrations of alkyl chain in SDS remains unchanged in two samples while there is reasonable shift in the a symmetric and asymmetric C-H scissoring vibrations of CH$_3$-N$^+$ moiety indicating the fact that capping of SDS on CdTe nanoparticles occurs via their head group [20].

The photocurrent density - voltage characteristics of a dye sensitized solar cell with and without SDS capped CdTe QDs are shown in Fig. 6(a). The optical current and voltage rise after loading the CdTe, as indicated in the figure. QDs, as well as the robust spectral linkage of the concurrent CdTe (CB) band levels as well as the dye (LUMO) longer optical path, lead to a faster injection of electrons into the TiO$_2$ conduction
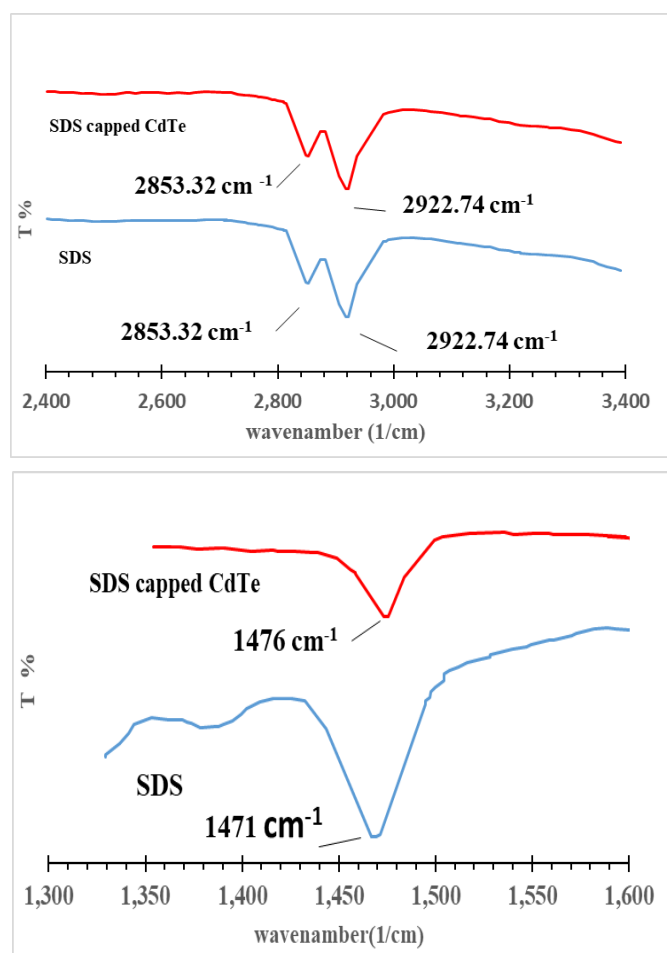

Fig. 5. FTIR spectra of SDS, SDS capped CdTe QDS in the range (a)2400-3400 cm^{-1}
(b) 1300-1600 cm^{-1}, respectively

band. [21] Fig. 6(b) depicts the corresponding power density as a function of voltage curve. The DSSC efficiency was estimated using the formula below.

$$\eta = \frac{J_{sc} V_{oc}\ FF}{P_{in}} \qquad (3)$$

Where: J_{sc}: The short-circuit current density, V_{oc}: The open-circuit voltage, FF: The Fill Factor of solar cell which is the ratio of ultimate power from the solar cell to the product of V_{oc} and I_{sc}, and P_{in}: The

power density of the incident light (100 mW/cm^2).

The transients of Open-Circuit Voltage decay (V_{OC}) of DSSCs with and without CdTe QDs are shown in Fig. 7(a). The V_{OC} response of the DSSC with QDs was significantly delayed compared to the DSSC without QDs. Indeed, the response of V_{OC} reveals a fall in electron concentration at the FTO surface caused by the charge re-combination technique, and so the faster response of the DSSC without QDs would be attributed mostly to the faster rate of charge re-combination. The measurement of transient V_{OC} has been developed.
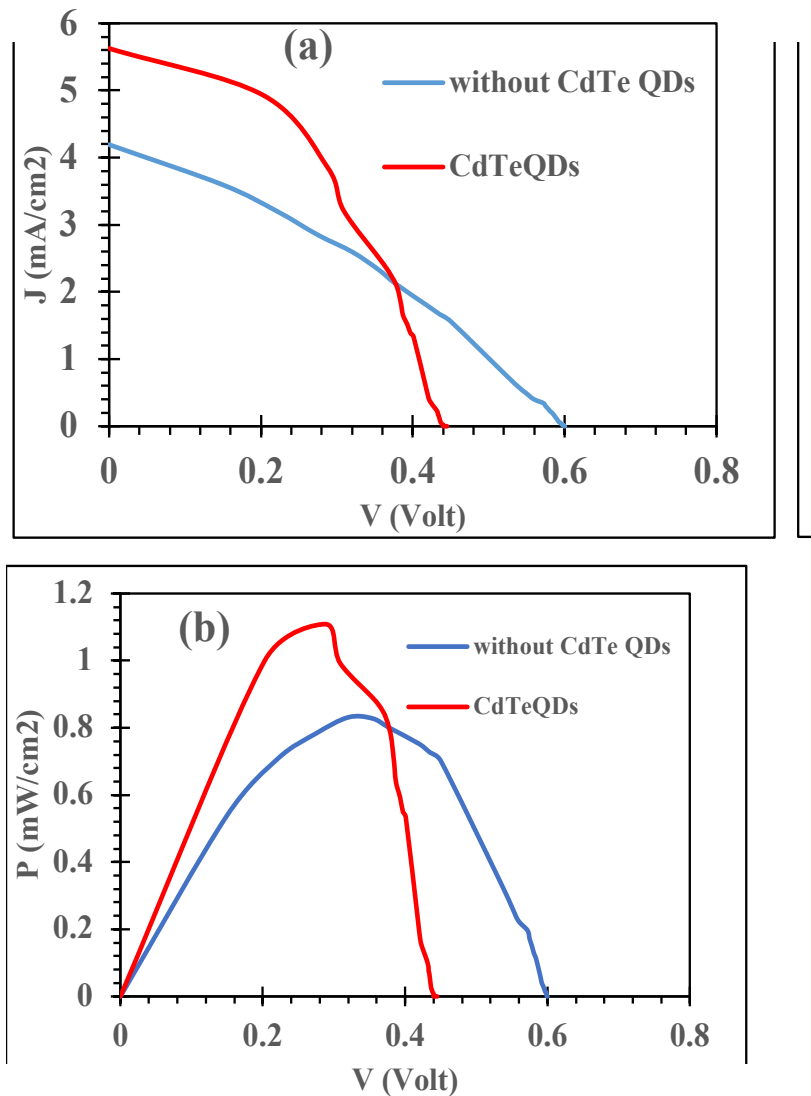

Fig. 6. (a) J-V characteristics of DSSC with and without SDS capped CdTe QDs and (b) power density in terms of voltage for DSSCs with as well as without SDS capped CdTe QDs.

used for calculating the lifetime (τn) of electron in Fig. 7(b) from the following equation ,The results are similar to what the researchers obtained [22]

$$\tau_n = -\frac{K_B T}{q}\left[\frac{dV_{oc}}{dt}\right]^{-1} \tag{4}$$

Where, K_B: The constant of Boltzmann, T: The absolute temperature, and Q: The elementary charge.

Fig. 8 depicts the semi-log plot of open-circuit voltage on the logarithm of xenon light intensity

based on the equation shown below [23].

$$V_{oc} = \frac{nk_B T}{q}\ln(I_0) \tag{5}$$

Where, n: The ideality factor, K_B: Boltzmann constant , T: Temperature, and q: The charge of electron.

Both DSSCs with and without SDS capped CdTe QDs exhibit ideal - diode behavior when their ideality factor value surpasses 2, as shown in Table 1, as predicted in DSSCs with n values
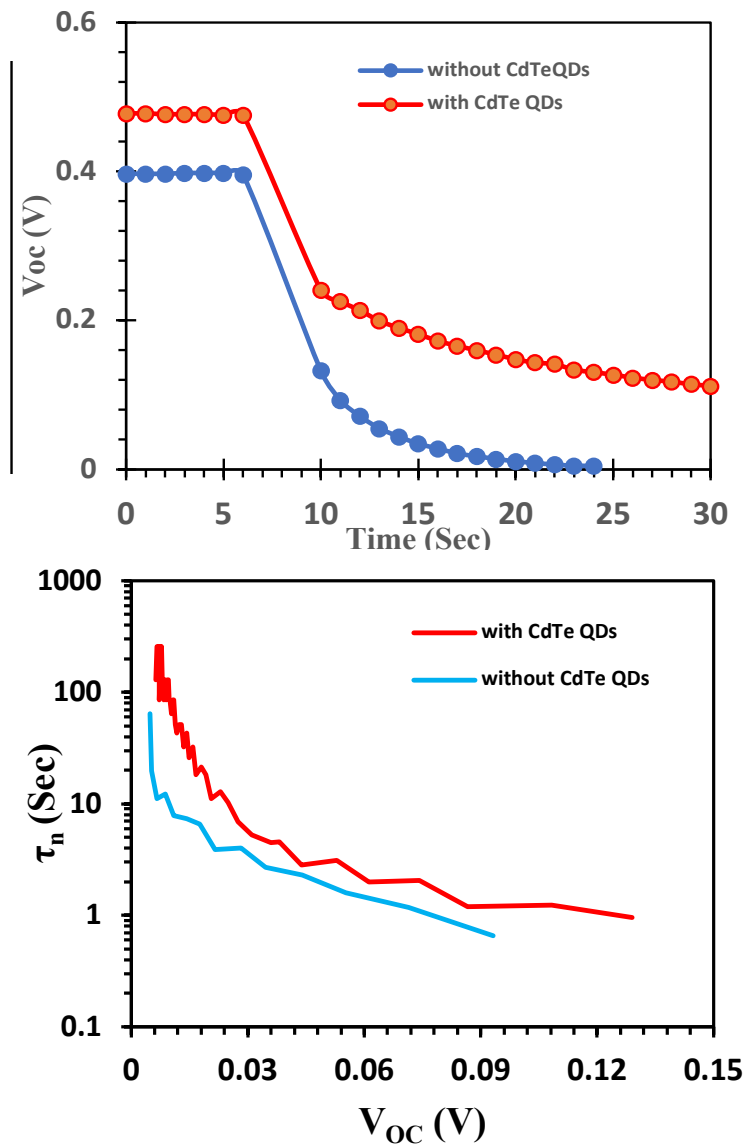

Fig. 7. (a) Transients of open-circuit voltage decay and (b) lifetime in terms of the open-circuit voltage for the DSSC without and with CdTe QDs
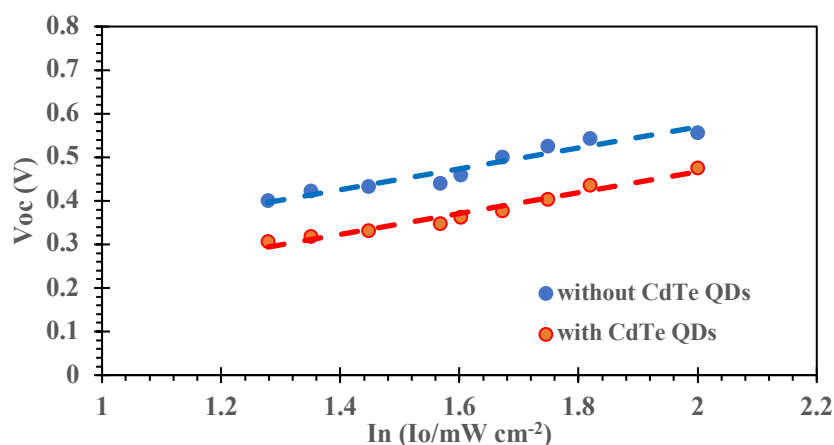
Fig. 8. Semi-log plot of open-circuit voltage as a function of light intensity for DSSC without and with SDS capped CdTe QDs.

Table 1. The photovoltaic characteristics of DSSCs with and without SDS-capped CdTe QDs.

DSSC	Voc (volt)	Jsc (mA/cm²)	F.F.	η %	n
Without SDS capped CdTe QDs	0.6	2.96	0.33	0.58	7.3
With SDS capped CdTe QDs	0.46	5.62	0.44	1.10	5.7

greater than 2, as opposed to silicon cells with n values between 1 and 2. When SDS capped CdTe QDs were added, the value of n dropped. Table 1 presents the photovoltaic properties of the DSSC. The results show that there is an improvement in the solar cell after adding SDS capped CdTe QDs.

CONCLUSION

The structural, morphological, and optical features of SDS-capped CdTe quantum dots were investigated utilizing a laser ablation approach. FTIR spectra investigation for SDS and SDS capped CdTe QDs verified the surfactant SDS capped CdTe QDs. The impact of loading SDS capped QDs in the Dye Sensitized solar cell was explored, and it was discovered that loading QDs improved photovoltaic characteristics. Jsc increased from 2.9 to 5.6 mA/cm2, and efficiency increased from 0.58% to 1.10% was that the results were good and similar to what is found in other research.

CONFLICT OF INTEREST

The authors declare that there is no conflict of interests regarding the publication of this manuscript.

REFERENCES

1. Hamakawa Y. Recent Progress of Amorphous-Silicon Solar-Cell Technology in Japan. International Journal of Solar Energy. 1982;1(1):33-53.
2. Maçaira J, Andrade L, Mendes A. Review on nanostructured photoelectrodes for next generation dye-sensitized solar cells. Renewable and Sustainable Energy Reviews. 2013;27:334-349.
3. Nideep TK, Ramya M, Kailasnath M. The influence of ZnS buffer layer on the size dependent efficiency of CdTe quantum dot sensitized solar cell. Superlattices Microstruct. 2019;130:175-181.
4. Elibol E, Elibol PS, Cadırcı M, Tutkun N. Improving the performance of CdTe QDSSCs by chloride treatment and parameter optimization. Mater Sci Semicond Process. 2019;96:30-40.
5. Nazeeruddin MK, Baranoff E, Grätzel M. Dye-sensitized solar cells: A brief overview. Solar Energy. 2011;85(6):1172-1178.
6. Elibol E, Tutkun N. Improving CdTe QDSSC's performance by Cannula synthesis method of CdTe QD. Mater Sci Semicond Process. 2019;93:304-316.
7. Gharibshahi E. Simulation, synthesis and optical properties of cadmium telluride (CdTe) semiconductor nanoparticles. Solid State Commun. 2020;320:114009.
8. Aramide G, Shona K, Keith B, Teresa B. IDENTIFY THE RISK TO HOSPITAL ADMISSION IN UK-SYSTEMATIC REVIEW OF LITERATURE. LIFE: International Journal of Health and Life-Sciences. 2016;2(2):20-34.
9. Xiao Z, Liu D, Tang Z, Li H, Yuan M. Synthesis and characterization of poly(lactic acid)-conjugated CdTe quantum dots. Mater Lett. 2015;148:126-129.
10. Gutiérrez HML, Solís-Pomar F, Gutiérrez-Lazos CD, Ruíz-Robles MA, Buitimea-Cantúa GV, del Angel- Sánchez K, et al. Forcespinning fabrication of CdTe-quantum dot/polylactic acid microfibers for novel surface-engineered application. Materials Research Express. 2021;8(9):096203.

11. Mohammed MA, Salman ON, Bülbül MM. Preparation of Ag@SiO$_2$ core–shell nanoparticles for plasmonic dye-sensitized solar cell application using laser ablation in liquid technique. Optical and Quantum Electronics. 2023;56(1).

12. Zhou FY, Hai H, Yuan YL, Li JP. Cover Picture: Ultrasensitive Electrochemiluminescence Biosensor for mRNA Based on Polymerase Assisted Signal Amplification (Electroanalysis 4/2017). Electroanalysis. 2017;29(4):937-937.

13. Khun Khun K, Mahajan A, Bedi RK. Effect of cationic/ anionic organic surfactants on evaporation induced self assembled tin oxide nanostructured films. Appl Surf Sci. 2011;257(7):2929-2934.

14. Kaur N, Bhullar V, Singh DP, Mahajan A. Bimetallic Implanted Plasmonic Photoanodes for TiO$_2$ Sensitized Third Generation Solar Cells. Sci Rep. 2020;10(1).

15. Tanvi T, Mahajan A, Bedi RK, Kumar S, Saxena V, Singh A, Aswal DK. Broadband enhancement in absorption cross-section of N719 dye using different anisotropic shaped single crystalline silver nanoparticles. RSC Advances. 2016;6(53):48064-48071.

16. Scherrer P. Bestimmung der inneren Struktur und der Größe von Kolloidteilchen mittels Röntgenstrahlen. Kolloidchemie Ein Lehrbuch: Springer Berlin Heidelberg; 1912. p. 387-409.

17. Langford JI, Wilson AJC. Scherrer after sixty years: A survey and some new results in the determination of crystallite size. J Appl Crystallogr. 1978;11(2):102-113.

18. Semaltianos NG, Logothetidis S, Perrie W, Romani S, Potter RJ, Sharp M, et al. CdTe nanoparticles synthesized by laser ablation. Appl Phys Lett. 2009;95(3).

19. Al-Heuseen K, Hashim MR. Synthesis and characterization of GaN thin films deposited on different substrates using a low-cost electrochemical deposition technique. AIP Conf Proc: AIP; 2012.

20. Abdel-Raouf N, Al-Enazi NM, Ibraheem IBM. Green biosynthesis of gold nanoparticles using Galaxaura elongata and characterization of their antibacterial activity. Arabian Journal of Chemistry. 2017;10:S3029-S3039.

21. Xiao J-W, Ma S, Yu S, Zhou C, Liu P, Chen Y, et al. Ligand engineering on CdTe quantum dots in perovskite solar cells for suppressed hysteresis. Nano Energy. 2018;46:45-53.

22. Yun J-H, Lyu M, Ahmed R, Triani G. Desirable TiO$_2$ compact films for nanostructured hybrid solar cells. Materials Technology. 2019;35(1):31-38.

23. Nedelcu D. Advanced Engineering Forum Vol.35. Advanced Engineering Forum: Trans Tech Publications Ltd; 2020.

24. Guillén E, Peter LM, Anta JA. Electron Transport and Recombination in ZnO-Based Dye-Sensitized Solar Cells. The Journal of Physical Chemistry C. 2011;115(45):22622-22632.